POLITECNICO
MILANO 1863

Spacecraft Attitude Dynamics
Final Project Report

Kiumars Askari

10656171

July 2021

Table of contents

1 Introduction

1.1 Project introduction

In this project we are supposed to model the attitude dynamics of a satellite orbiting the earth, we will include the simulation of sensors and actuators in this model. The shape and size of the satellite and the orbit is not specified but it is mandatory to use specific sensors and actuators. We will justify any additional parameter utilized in the simulation. All the simulations regarding the project have been done using Simulink.

1.2 Individual specifications

In this project, the following specifications were necessary to be implemented in the Simulink blocks:

Table 1-1 Individual specifications required to be modeled in the project.

Attitude parameters	Attitude sensors	Attitude actuators
Euler Angles	**Star sensor**	**3 Magnetic coils and 1 Reaction wheel**

2 Satellite and Orbit characteristics

In the purpose of choosing the right specifications for the satellite and the orbit, a particular satellite with the same sensor specification was found. The Astronomical Netherlands Satellite (ANS) was a space-based telescope. It had an initial orbit with a periapsis of 266 kilometers, an apoapsis of 1176 kilometers, and an inclination of 98 degrees. This orbit is sun-synchronous, and the attitude of the spacecraft could be controlled through reaction wheels. The momentum stored in the wheels throughout the orbit was occasionally dumped via magnetic coils interacting with the earth's magnetic field.

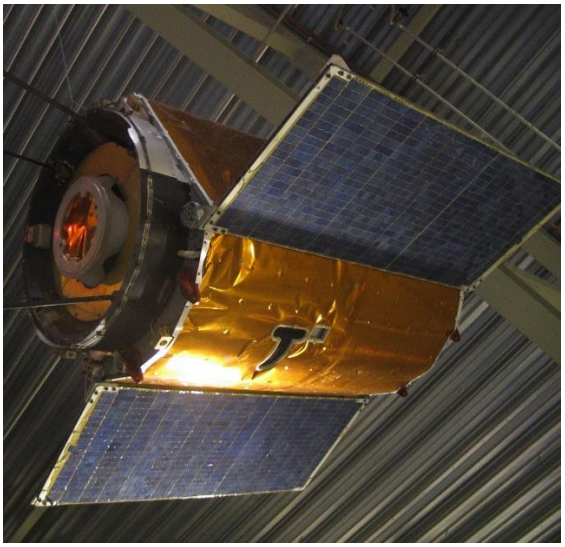

Figure 2.1 ANS satellite model used for this simulation.

Table 2-1 Classical Keplerian elements of the sample orbit, based on ANS data

Semi-major axis [km]	Eccentricity	Inclination [deg]	Right ascension [deg]	Argument of perigee [km]	Initial true anomaly [deg]
7092	**0.0641568**	**98**	**Depends on Time**	**0**	**270**

Table 2-2 Data taken from the ANS

Main Body Mass [kg]	9
Main Body Dimensions [m]	0.1 x 0.2 x 0.3
Solar Panels Mass [kg]	0.6
Solar Panels Dimensions [m]	0.2 x 0.3
Pointing objective	3-axis, Earth nadir pointing
Desired Pointing accuracy [deg]	< 1.00

The satellite body is simulated as a rectangular cube with two solar panels attached to one end. As you can see, since the orbit is sun-synchronous, the right ascension of the ascending node depends on the time of year, which is calculated accordingly in the simulation. The initial true anomaly is set to 270 degrees, because at this position in the 21st of March, even starting the simulation with body and the inertial frame overlapping, will give us a good accuracy towards Earth-Pointing.

Table 2-3 Moments of Inertia

I_x [kg.m^2]	I_y [kg.m^2]	I_z [kg.m^2]
0.1585	**0.0921**	**0.0866**

3 Space environment and disturbances

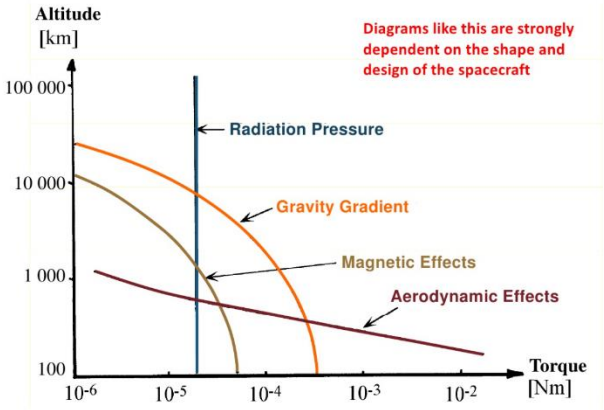

Figure 3.1 Typical magnitude of disturbing torques [4]

In what follows we'll break down all the components that compose the environmental effects and disturbances on the satellite. It's important to note that due to the reasonably low altitude of the satellite, we can neglect the third body perturbations due to the moon's gravity.

3.1 Gravity gradient perturbations

If the orientation of the satellite is not symmetrical with respect to its position vector connected to the center of Earth, the satellite will experience gravity gradient perturbation torques. For gravity gradient stability, the body axis with the minimum moment of inertia should be pointed towards Earth.

$$\boldsymbol{T_{d_{GG}}} = \frac{\boldsymbol{3\mu_E}}{|\boldsymbol{r_{SC}}|^3}\begin{bmatrix}(\boldsymbol{I_z}-\boldsymbol{I_y})\boldsymbol{c_2c_3}\\(\boldsymbol{I_x}-\boldsymbol{I_z})\boldsymbol{c_1c_3}\\(\boldsymbol{I_y}-\boldsymbol{I_x})\boldsymbol{c_2c_2}\end{bmatrix} \quad \textbf{(3-1)}$$

3.2 Magnetic perturbations

Since the altitude is low, the magnetic field cannot be implemented as a simple magnetic dipole. We can use an order 13 IGRF magnetic field but since Simulink already has a built-in function for calculating the Earth magnetic field, we'll use the "World Magnetic Model" block. Due to the electronics and the wirings, there is always a residual dipole generated inside the satellite. This residual dipole will interact with the magnetic field of the Earth and create a torque that will affect the attitude of the satellite. Determining the residual dipole at the preliminary stage of the spacecraft design is extremely hard. So it is best to consider the worst case scenario, and for a satellite this size, we can assume the residual dipole to be a white noise with the power of 0.1 A.m^2. The corresponding disturbance torque will be calculated from the equation below.

$$\boldsymbol{T_{d_{MGN}}} = \boldsymbol{m_{res}} \times \boldsymbol{b} \quad \textbf{(3-2)}$$

3.3 Aerodynamic drag perturbations

Satellites in LEO will experience the drag torques on the spacecraft's body. For this project since the altitude changes drastically and so does the air density, we will use the "ISA Atmosphere Model" block to estimate the more precise value of air density based on the current altitude during the simulation. In this project, 6 surfaces of the satellite and their respective normal vectors are modeled. The position of the center of each surface with respect to the center of mass of the whole body has also been stored in the matrix. C_D has been assumed to be 2.2 for this simulation.

$$\boldsymbol{T_{d_{DRG}}} = \sum_{\boldsymbol{i=1}}^{\boldsymbol{N}} \boldsymbol{r_i} \times \boldsymbol{F_i} \quad \textbf{(3-3)}$$

where

$$\boldsymbol{F_i} = \begin{cases} -\frac{\mathbf{1}}{\mathbf{2}}\boldsymbol{\rho_{atm}C_D v_{rel}^2}\frac{\boldsymbol{v_{rel}}}{\|\boldsymbol{v_{rel}}\|}(\widehat{\boldsymbol{N}}_{\boldsymbol{bi}}\cdot\frac{\boldsymbol{v_{rel}}}{\|\boldsymbol{v_{rel}}\|}) & \textbf{when } \widehat{\boldsymbol{N}}_{\boldsymbol{bi}}\cdot\frac{\boldsymbol{v_{rel}}}{\|\boldsymbol{v_{rel}}\|} > \mathbf{0} \\ \mathbf{0} & \textbf{when } \widehat{\boldsymbol{N}}_{\boldsymbol{bi}}\cdot\frac{\boldsymbol{v_{rel}}}{\|\boldsymbol{v_{rel}}\|} < \mathbf{0} \end{cases}$$

And $\mathbf{r_i}$ is the position vector from the center of mass of the satellite to the center of the specific surface. The relative velocity can also be attained by having the velocity vector of the satellite, subtracted by the atmosphere velocity at the position of the satellite, all transformed back to the body frame.

3.4 Solar radiation pressure perturbations

The direct solar radiation intensity for orbits around the Earth can be assumed constant and equal to 1358 $\frac{W}{m^2}$. During the satellite being in sunlight, this solar radiation pressure will apply forces on the surfaces of the satellite that will create a disturbance torque, if the geometrical center is not coincident with the center of gravity of the satellite. The specular and diffusive reflection coefficients of the satellite surfaces are provided in Table 3-1.

Table 3-1 Specular and diffusive reflection coefficients of the satellite surfaces

End faces		Solar cell covered body faces	
$\boldsymbol{\rho_s}$	$\boldsymbol{\rho_d}$	$\boldsymbol{\rho_s}$	$\boldsymbol{\rho_d}$
0.5	**0.1**	**0.0**	**0.0**

The solar radiation pressure torques can be calculated as below:

$$\boldsymbol{T_{d_{SRP}} = \sum_{i=1}^{N} r_i \times F_i} \quad \textbf{(3-7)}$$

where $\mathbf{r_i}$ is the position of the center of pressure (area) of the surface **i** with respect to the center of gravity and the force is equal to:

$$\boldsymbol{F_i} = \begin{cases} \boldsymbol{-A_i P(\hat{n}_i \cdot \hat{s})\left[(1-\rho_s)\hat{s} + 2\left(\rho_s(\hat{n}_i \cdot \hat{s}) + \frac{\rho_d}{3}\right)\right]} & \textbf{when } \boldsymbol{\hat{n}_i \cdot \hat{s} > 0} \\ \boldsymbol{0} & \textbf{when } \boldsymbol{\hat{n}_i \cdot \hat{s} < 0} \end{cases}$$

Since the radiation of Earth is neglected, the satellite will experience no radiation pressure torque during its eclipse phase of the orbit.

4 Selecting ADCS components

With the aim of controlling the attitude of the satellite, and considering the mandatory requirements for the project, the following parts are chosen:

4.1 Attitude sensors

To determine the orientation in space, at least two direction vectors that are not parallel to each other are required to be identified by the sensors onboard the satellite. However, only two sensors will not be enough since there is the possibility of failure of one sensor or alignment of the sensed direction vectors.

4.1.1 Horizon (Earth) sensors

In the simplified model, horizon sensors can determine the direction of the center of Earth in the body frame. Infra-red horizon sensors can provide the Earth direction also in eclipse and they can have small sizes. Thus, in this project, it is considered to have several IR horizon sensors on each face of the satellite's central body to provide constant data of the Earth's direction vector.

Table 4-1 Horizon sensor specifications. Data were taken from MAI-SES (Maryland Aerospace, Inc.)

Sensor update rate	Sensor potential accuracy
100 [Hz]	**0.25 [degrees]**

4.1.2 Sun sensors

Sun sensors typically have a small size and multiple sensors are mounted on every surface of the central body. The sun sensors only work when the satellite is in sunlight and do not give the position of the sun with respect to the body frame during the eclipse. It should be considered to have several sun sensors on each body surface to always have the sun position vector when the satellite is in sunlight.

Table 4-2 Sun sensor specifications. Data were taken from SS200 (Hyperion Technologies, B.V.)

Sensor update rate	Sensor potential accuracy
100 [Hz]	**0.5 [degrees]**

4.1.3 Magnetometers

Magnetometers give the direction and magnitude of Earth's magnetic field at the position of the satellite in orbit, in the body frame. Magnetometers are paired with magnetorquers for attitude control. Realistically, magnetometers will not be as effective to be used for altitudes more than 6000 kilometers [2]. Since the satellite will be orbiting at a low altitude, the use of magnetometers may be advantageous.

Table 4-3 Magnetometer specifications. Main data are taken from Nanosense M315, however potential accuracy is taken from the literature [4] [2] [7]

Sensor update rate	Noise	Sensor potential accuracy
140 [Hz]	**15 [nT]**	**1 [deg]**

4.1.4 Gyroscopes

The gyroscopes can provide the angular velocity of the satellite, in the body frame. The problem with gyroscopes is that they have a bias noise error in their output and that gets accumulated through time and needs to be reset. However, since the duration of this simulation is short, the resetting will be neglected. By taking a generic direction in the body frame and by cross producting and integrating the value with the angular velocities sensed by the gyroscopes, it is possible to have a roughly estimated direction vector that can be used in attitude determination.

Table 4-4 Gyroscope specifications. Data were taken from Sensonor STIM300 of the slides [4]

Sensor update rate	Angular random walk	Rate random walk
262 [Hz]	**0.15 [deg/hr$^{0.5}$]**	**0.0003 [deg/hr$^{1.5}$]**

4.2 Attitude determination method

In practice, to have the best possible attitude determination while accounting for the errors in the sensor data, algebraic methods will not be used and Wahba's problem will be considered. In this project, to have fast calculations and avoid optimized minimization, the analytical solution to the Wahba problem shall be employed by using the singular value decomposition. For this means, it is assumed that the sensors give the direction of the Sun, the Earth, the magnetic field, and/or a generic inertial direction vector, in the body frame. The accuracy of each sensor will be the main criteria for the selection of the weighting factor of each sensed direction in the cost formula.

For this model, two different sets of direction vectors will be the input of the attitude determination block. One is when the satellite is sunlight. In this case, the Sun direction, the Earth

direction, and the magnetic direction can be used to obtain the transfer matrix used in attitude determination. On the other hand, when the satellite is in eclipse, the Sun direction will not be available, and using only two vectors for the Wahba's problem will give highly noised results. To compensate for this matter, right before the eclipse, a generic inertial direction is taken and transferred to the body frame. Then, by using the angular velocity sensed by the gyroscope, the generic direction will be propagated in the body frame during the eclipse and will be used as the third direction vector in the Wahba's problem.

$$\mathbf{B} = \sum_{i=1}^{N} \boldsymbol{\alpha_i s_{bi} v_{Ni}^T} \tag{4-1}$$

And then with the SVD of B, it is driven:

$$\boldsymbol{A_{B/N} = UMV^T} \tag{4-2}$$

Where matrix **U** is the eigenvectors of matrix $\mathbf{BB}^T$ and **V** is the eigenvectors of matrix $\mathbf{B}^T\mathbf{B}$. Matrix **M** will be a diagonal matrix with diagonal values of [1 1 det(**U**)*det(**V**)]. The final goal of the attitude determination is to achieve $\mathbf{A_{B/N}}$ which is the transformation matrix of the inertial to the body frame.

Regarding the filtering, since the modeling of the satellite is carried out simply, and the controlling of the CubeSat will not be very fast, simple Butterworth low-pass filters will be used for the output of the gyroscope and the attitude determination block, but only to the first degree to avoid too much phase delay.

4.3 Orbit, Dynamics, and Kinematics model of the satellite

4.3.1 Orbit

To propagate the orbit, two main methods are available. Either with the given initial Keplerian elements, the position and velocity of the spacecraft in the inertial frame can be obtained using a Keplerian to Cartesian transformation, or the radius and the rate of true anomaly change are introduced in the LVLH or better yet the orbital reference frame, and then with rotating the coordinate system, the inertial values for the position and velocity vector can be obtained. In modeling the orbit in this simulation, the latter method is used.

$$\boldsymbol{r = \frac{a(1-e^2)}{1+e\cos\theta}} \qquad \boldsymbol{\dot{\theta} = \frac{\sqrt{\frac{\mu}{a^3}}(1+e\cos\theta)^2}{(1-e^2)^{1.5}}} \tag{4-3}$$

If the LVLH frame is considered, then the radius will be in the $[1\ 0\ 0]^T$ direction. The transformation matrix from LVLH to the inertial frame will be carried out with three transformation rotation matrices.

$$\boldsymbol{A_{N/L} = R_3(-\Omega)R_1(-i)R_3(-\omega-\theta)} \tag{4-4}$$

Given the initial date and time, the initial angular position of Earth with respect to the inertial frame (ECEF to ECI) is calculated at the beginning and then propagated with respect to the time of the simulation. The position of the Sun is also obtained through the use of the Ephemerides program and

by calculating the position of Earth with respect to the Sun in the ecliptic plane, and then transforming the opposite direction to the inertial frame. With having the direction of the Sun, and considering a spherical Earth with a cylindrical shadow, the eclipse times of the satellite's orbit can also be calculated.

It is worth mentioning that due to this satellite's orbit being sun-synchronous we will rotate the right ascension of the ascending node by the angular velocity of the earth around the sun which is because of the J2 effects. But we will neglect the other effects on the orbit and we assume that the other perturbations only affect the attitude of the satellite.

4.3.2 Dynamics

With assuming the body frame for the satellite as the principal axes with the principal inertia moments in those directions, the dynamics of the satellite can be obtained as below.

$$\begin{cases} \dot{\omega}_x = \dfrac{I_y - I_z}{I_x}\omega_y\omega_z + \dfrac{T_{c_x}T_{d_x}}{I_x} \\ \dot{\omega}_y = \dfrac{I_z - I_x}{I_y}\omega_y\omega_z + \dfrac{T_{c_y}T_{d_y}}{I_y} \\ \dot{\omega}_z = \dfrac{I_x - I_y}{I_z}\omega_y\omega_z + \dfrac{T_{c_z}T_{d_z}}{I_z} \end{cases} \quad \textbf{(4-5)}$$

4.3.3 Kinematics

It was mandatory to use the Euler angles for this project. The tricky part about using the Euler angles is to avoid the singularity which is the result of the second angle reaching 90 degrees. Now by looking closely at the orbit and the desired orientation of the satellite we can safely choose the 321 order of rotations. The reason is that in the orbit, if we want to point the Z axis of the satellite towards the earth and the X axis towards the sun, then the angle of the Y axis will be more or less consistent.

The 321 order rotation matrix and the angle rate equations can be written using the below matrices:

$$\begin{bmatrix} c\theta_2 c\theta_1 & c\theta_2 s\theta_1 & -s\theta_2 \\ s\theta_3 s\theta_2 c\theta_1 - c\theta_3 s\theta_1 & s\theta_3 s\theta_2 s\theta_1 + c\theta_3 c\theta_1 & s\theta_3 c\theta_2 \\ c\theta_3 s\theta_2 c\theta_1 + s\theta_3 s\theta_1 & c\theta_3 s\theta_2 s\theta_1 - s\theta_3 c\theta_1 & c\theta_3 c\theta_2 \end{bmatrix}$$

$$\frac{1}{c\theta_2}\begin{bmatrix} 0 & s\theta_3 & c\theta_3 \\ 0 & c\theta_2 c\theta_3 & -c\theta_2 s\theta_3 \\ c\theta_2 & s\theta_2 s\theta_3 & s\theta_2 c\theta_3 \end{bmatrix}$$

The first matrix is the rotation matrix and the second one multiplied by the body angular velocities will give the Euler angle rates.

4.4 Attitude control algorithm

There are two different control methods that can be used after orbit injection which will be explained in what follows.

4.4.1 De-tumbling phase

In this phase we will try to make the satellite stationary with respect to the inertial frame.

$$\mathbf{M}_{Ci} = \boldsymbol{k_i \omega_i} \tag{4-6}$$

$$\mathbf{d} = \frac{\boldsymbol{B \times M_c}}{\boldsymbol{B^2}} \tag{4-7}$$

$$\boldsymbol{M_{eff_{MAG}}} = \frac{\mathbf{1}}{\boldsymbol{B^2}}(\boldsymbol{B \times M_c}) \times \boldsymbol{B} \tag{4-8}$$

So for the Earth-Pointing phase we will assume the satellite to be more or less stationary with respect to the inertial frame and then will begin the simulation.

4.4.2 Earth nadir pointing phase

The mission is to point the Z axis of the satellite towards the center of the Earth while trying to point the solar panels towards the sun which means we are at the same time trying to make the X axis and the direction of the sun in the body frame, close to each other. The target transfer matrix can be calculated as follows:

$$\begin{cases} \boldsymbol{Z = A_{IL}} \begin{bmatrix} \mathbf{1} \\ \mathbf{0} \\ \mathbf{0} \end{bmatrix} \\ \boldsymbol{v = S_I - \frac{S_I . Z}{|Z|^2} Z} \\ \boldsymbol{X = \frac{v}{|v|}} \\ \boldsymbol{Y = Z \times X} \end{cases} \tag{4-10}$$

$$A_T = \begin{bmatrix} X_I^T \\ Y_I^T \\ Z_I^T \end{bmatrix}$$

$$A_e = A_s A_T'$$

The goal of the linear control law is to have the $\mathbf{A_e}$ matrix tend towards the identical matrix. Meaning that the off-diagonal elements should move towards zero. By having the $\mathbf{A_e}$ matrix components, and by assuming a linear PD for the control torque, the calculation of the required torque in each direction will be as follows:

$$\begin{cases} M_x = \frac{k_{px}}{2}(a_{23} - a_{32}) + k_{dx}(\omega_x - \omega_{req_x}) \\ M_y = \frac{k_{py}}{2}(a_{31} - a_{13}) + k_{dy}(\omega_y - \omega_{req_y}) \\ M_z = \frac{k_{pz}}{2}(a_{12} - a_{21}) + k_{dz}(\omega_z - \omega_{req_z}) \end{cases} \quad \textbf{(4-11)}$$

Where the a_{ij} are the elements of the *i*th row and *j*th column of the error matrix. Since the LVLH frame is also rotating with respect to the inertial frame, the components of the required nominal angular velocity have also been added to the control law.

4.5 Actuator

In this part, we'll discuss the specifications of the actuators used in the simulation.

4.5.1 Magnetorquers

For the reasons mentioned, the following component has been selected as magnetorquer in all 3-axes.

Table 4-5 Magnetorquer specifications. Main data are taken from CubeTorquer & CubeCoil by CubeSpace [9]

Actuator action rate	Maximum moment	Residual moment
10 [Hz]	**1.5 [A.m^2]**	**0.00048 [A.m^2]**

4.5.2 Reaction wheels

Three reaction wheels shall be used instead of one, to be able to compensate for the magnetorquers whenever needed and to also distribute the momentum required in the third axis, between 3 different wheels, delaying the wheel from reaching the saturation point.

Table 4-6 Reaction wheel specifications. Main data are taken from small size CubeWheel by CubeSpace [10]

Actuator action rate	Maximum angular velocity	Maximum error in angular velocity	Moment of Inertia	Max RPM rate
1 [Hz]	**8000 [RPM]**	**5 [RPM]**	**1e-5 [kg.m^2]**	**100 [RPM/sec]**

The three reaction wheels will be placed in each of the main axes of the body.

5 Simulink modeling

As you can see in the figure below, each block has been separated by using a subsystem to simplify the graph. By double-clicking on each graph, you'll see a window that inputs related to that specific block can be given.

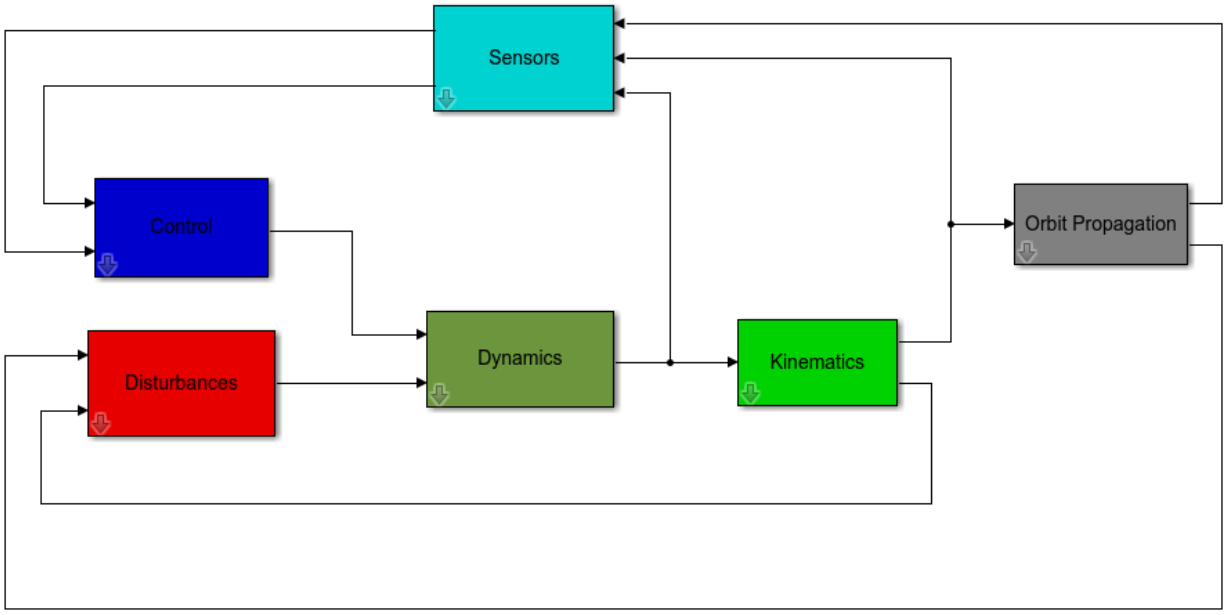

Figure 5.1 Oversimplified block diagram of the Simulink model

Each of the blocks in Figure 5-1 has a complicated composition of several subsystems. As an example, a simplified model of the Disturbances block can be seen below:

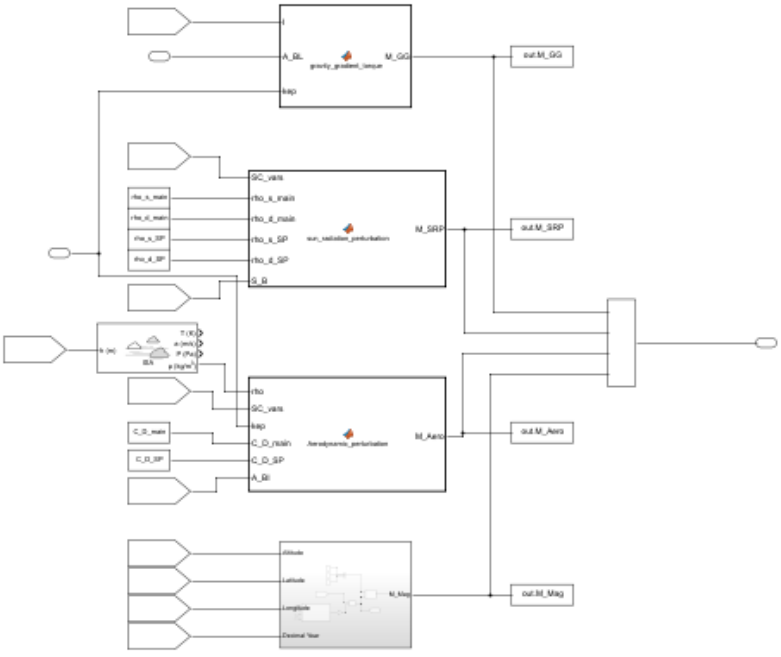

Figure 5.2 Inside the Disturbances block

An example of the input window for the Control block is also seen in the figure below:

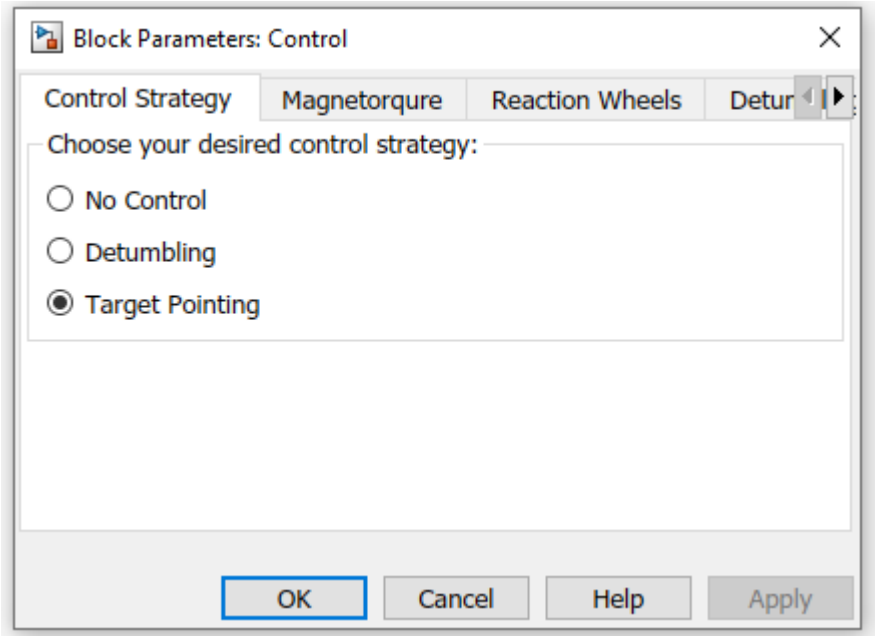

Figure 5.3 Example of the input window of Control block

As you can see, in this input window, it's possible to choose the control strategy, the magnetorquers, reaction wheels and the control law parameters.

6 Results

Simulation for the detumbling of the satellite was done for around 5000 seconds is nearly the orbit period of the satellite. With an initial angular velocity of 5 deg/sec in each direction, the disturbance torques are shown in the figure below:

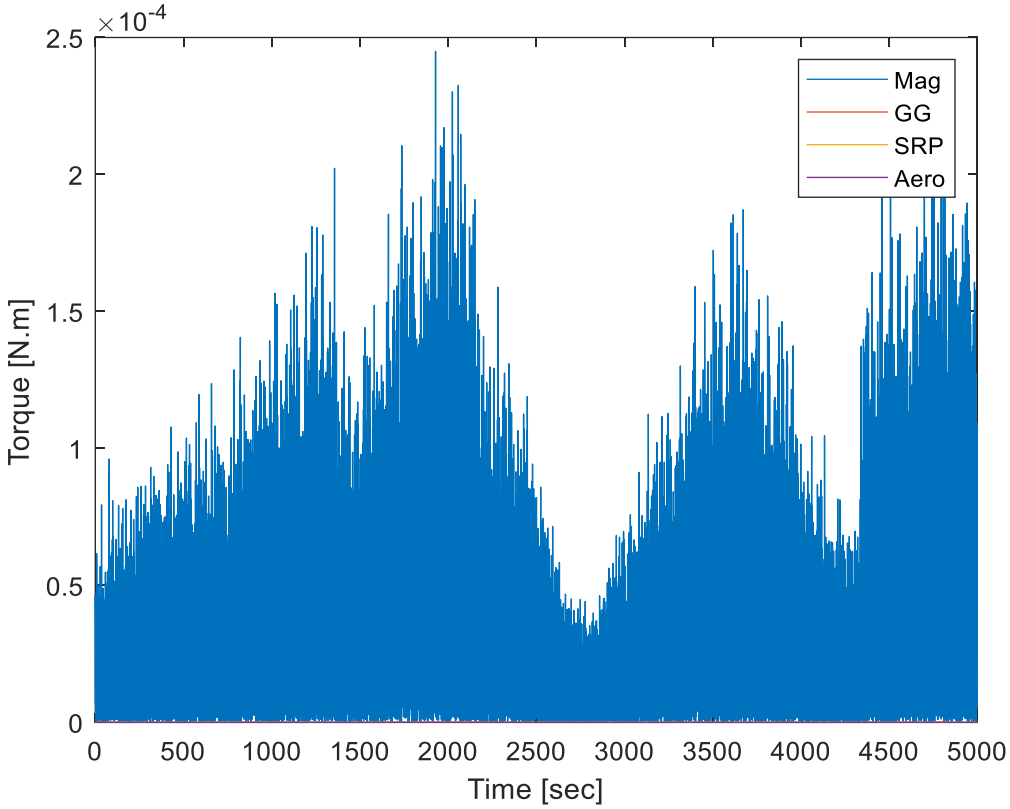

Figure 6.1 Disturbance torques on a control-free CubeSat

The mean value for the SRP disturbance is 3.21e-8, for the Gravity Gradient it's 2.02e-8, for Aerodynamic disturbances it's 2.40e-15 and for the Magnetic disturbances it's 3.38e-5, all in N.m unit. As you can see in the following figure, the angular velocities in the body frame are nearly coming to zero as a result of detumbling.

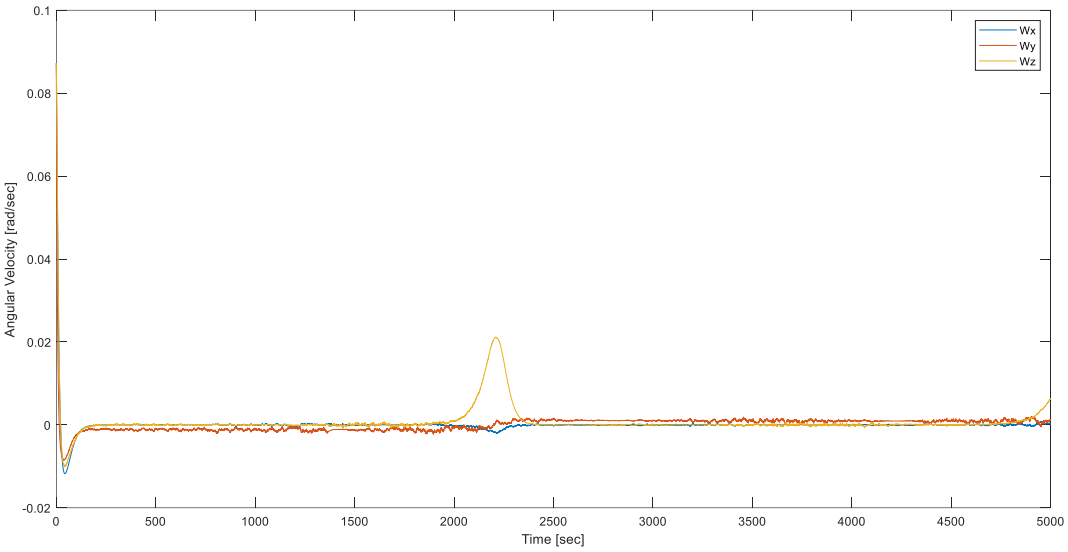

Figure 6.2 Angular velocity progression of the CubeSat

The Euler angles during this time are shown in this figure:

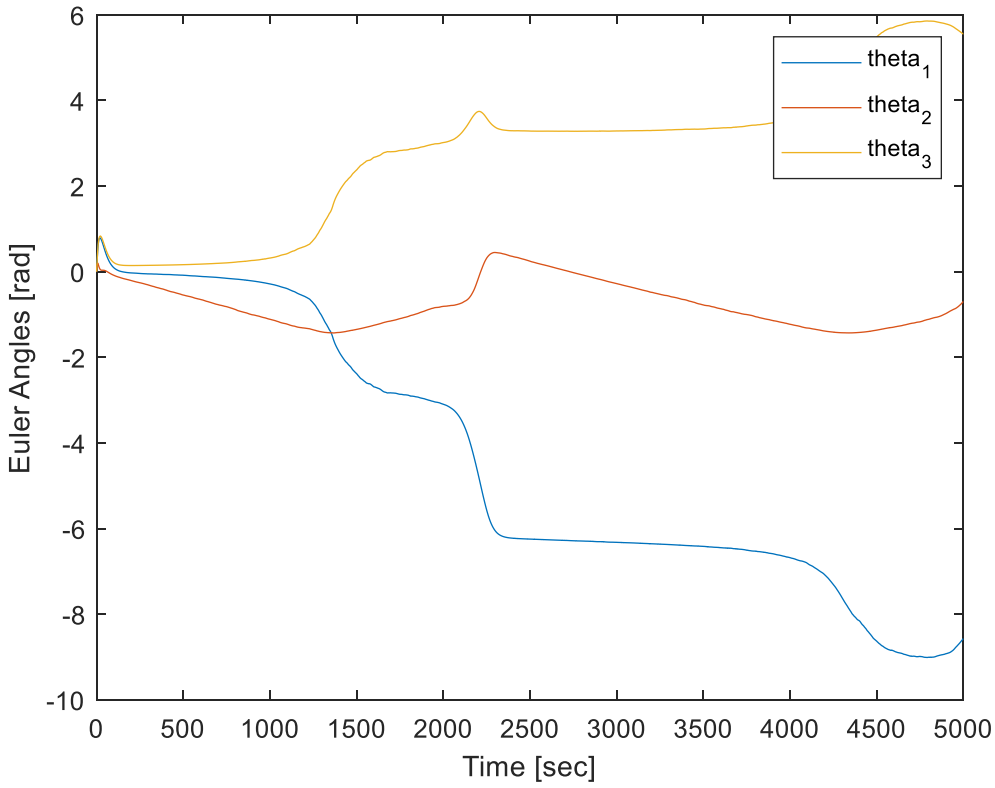

Figure 6.3 Euler Angles

However it is evident that due the use of less accurate control method which is magnetic, in two axes, there are still residual angular rates in the body that result in the constant change in Euler angles. But for the purpose of detumbling which will result in a more accurate form of control in the Earth Pointing phase, this accuracy is sufficient in the first 200 seconds of detumbling, because we don't use it for long durations of time, due to inevitable losses in accuracy.

Now in this next part, we'll see the effect of Earth Pointing. For this purpose we give an initial angular velocity of 0.5 deg/sec in each direction because we are assuming a detumbled state for the satellite. Also we give 10 deg deviation from the inertial frame in each Euler angle.

The earth pointing results are shown in the figures below:

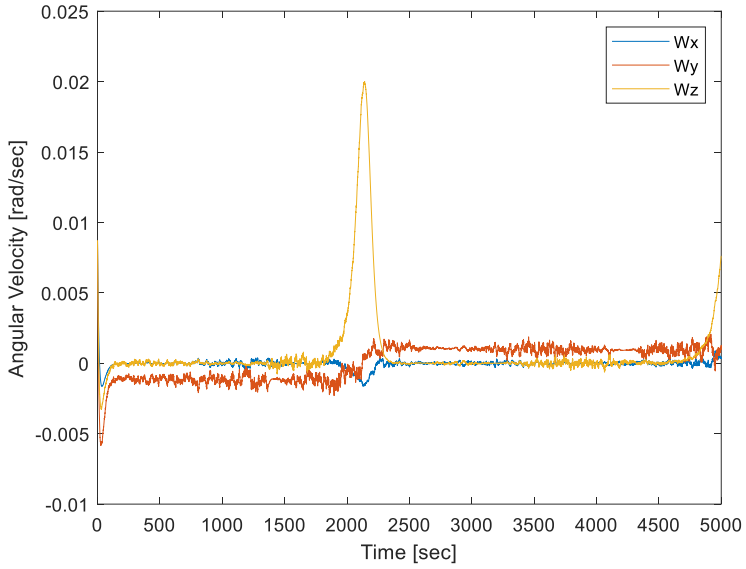

Figure 6.5 Angular Velocities

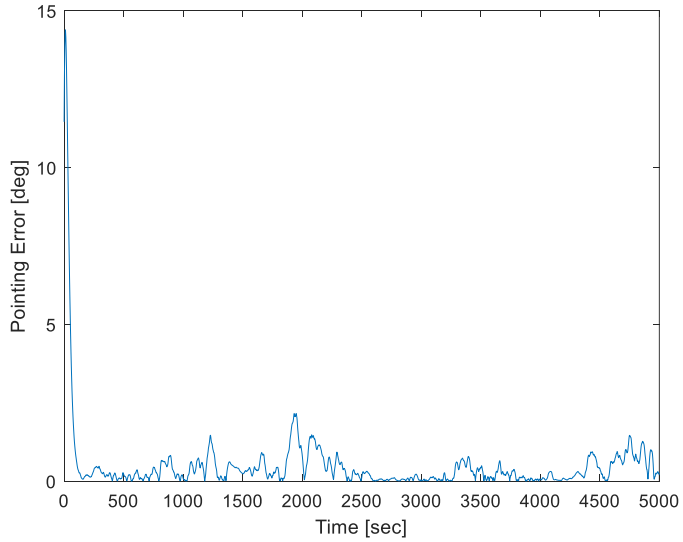

Figure 6.6 Pointing Error

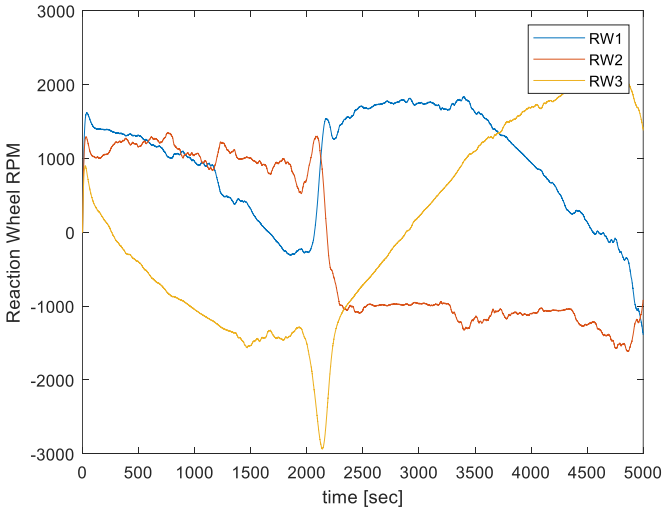

Figure 6.7 Reaction Wheels RPM

As it can be seen, the pointing error for the majority of the orbit period remains around 1 deg which is acceptable. Also we can see that the reaction wheels are not being saturated which means the control law that is considered is desirable.

7 Bibliography

[1] D. Gerhardt, M. Bisgaard, L. Alminde and e. al., "GOMX-3: Mission Results from the Onaugural ESA In-Orbit Demonstration CubeSat," in *30th Annual AIAA/USU Conference on Small Satellites*, 2016.

[2] L. J. Wiley and J. R. Wertz, Space Mission Analysis and Design, Microcosm Press and Kluwer Academic Publishers, 1999.

[3] J. Davis, "Mathematical modeling of Earth's magnetic field - Technical note," Blacksburg, 2004.

[4] F. Bernelli, *Spacecraft Attitude Dynamics Lecture Slides*, Politecnico di Milano, 2020.

[5] A. M. Aerospace, *MAI-SES IR Earth Horizon sensor - Specifications brochure.*

[6] SOLARMEMS, *nanoSSOC-D60 datasheet,* 2016.

[7] Gomspace, *Nanosense M315 datasheet,* 2019.

[8] Arianespace, *Vaga user's manual*, 2014.

[9] CubeSpace, *CubeTorquer & CubeCoil brochure.*

[10] CubeSpace, *CubeWheel brochure.*

[11] B. Dachwald, "Spacecraft Attitude Determination and Control," 2009. [Online]. Available: https://www.slideshare.net/abi3/bsf08-spacecraft-attitude-determination-and-control-v1-0. [Accessed February 2021].